**X-ray scattering & crystals Physics 617, Feb. 1, 2017 J. H. Ross**

X-ray diffraction, as well as neutron and electron scattering techniques, play a large role in characterizing crystalline (and even non-crystalline) materials, although the instrumentation has advanced considerably since the discussion chapter 6 in the text were written. Xray scattering has also played an important historical role in the formulation of our reciprocal-space understanding of crystals, and we will use these concepts throughout the course.

**Notes on techniques:** *X-rays* occupy the part of the electromagnetic spectrum appropriate for studying typical crystal lattices, with wavelength somewhat less than the Bragg-plane spacings. While x-ray studies are often performed on relatively small instruments, *neutron* scattering requires going to a centralized facility, and there are currently about 10 neutron scattering facilities in the US, for example the large facilities at Oak Ridge and NIST. Although the instrumentation is rather different, the results for *elastic* neutron scattering can be in many ways quite similar to x-ray scattering results, and the description below also applies. However note also that *inelastic* neutron scattering is also well established as a sensitive probe for excitations such as phonons and magnons, but this will be discussed later (phonon scattering in chapter 24). *Electron* beams have a smaller penetration depth than neutrons or x-rays, so it is more difficult to extract high-resolution crystal parameters from electron diffraction. However in a *transmission-electron electron microscope* (TEM; there are several of these instruments on our campus), the beam can be focused on nano-scale crystallites and particles, and electron scattering is particularly useful for such situations. New developments in TEM in recent years have led to sub-Ångstrom resolution, allowing the imaging of even individual atoms and defects. Somewhat different electron scattering setups are commonly used for surface-science and in epitaxial deposition systems, for example *Low Energy Electron Diffraction*. While *X-ray* scattering systems can be standard laboratory instruments as noted above (there are many of these on campus, both for powder and single crystals), extremely high resolution studies can be carried out at synchrotron radiation facilities and other specialized light sources (for example the Advanced Light Source at Lawrence Berkeley Lab and National Synchrotron Light Source at Brookhaven). These can allow structure refinement for extremely large macromolecules. The high resolution of these machines in recent years has also allowed *inelastic x-ray scattering* to be exploited for the study of excitations in solids. Finally, there are also scanning tunneling microscopy (STM), and other scanning probe techniques (SPM = scanning probe microscopy), that have also been developed since the publication of our text. Together, all of these techniques now allow for the imaging and analysis of crystal structures of materials in a much more routine way.

As an example of diffraction results, see Figure 1. This figure came from a publication our of my lab on cage-structured thermoelectric materials, and it serves to illustrate characteristic results for powder and single crystal samples; at the end of these notes is a short description of these methods. The main part of the top figure is an powder x-ray diffraction spectrum, for the structure shown in the inset, a silicon clathrate. The relative intensities of the peaks could also be calculated based on the positions and identities of the basis atoms, which is the red curve, and the lowest curve in that plot shows the small differences between the data and the fit. At the bottom

of the figure are electron diffraction images taken from three small crystallites, showing the characteristic single-crystal peaks as observed in such a TEM measurement.

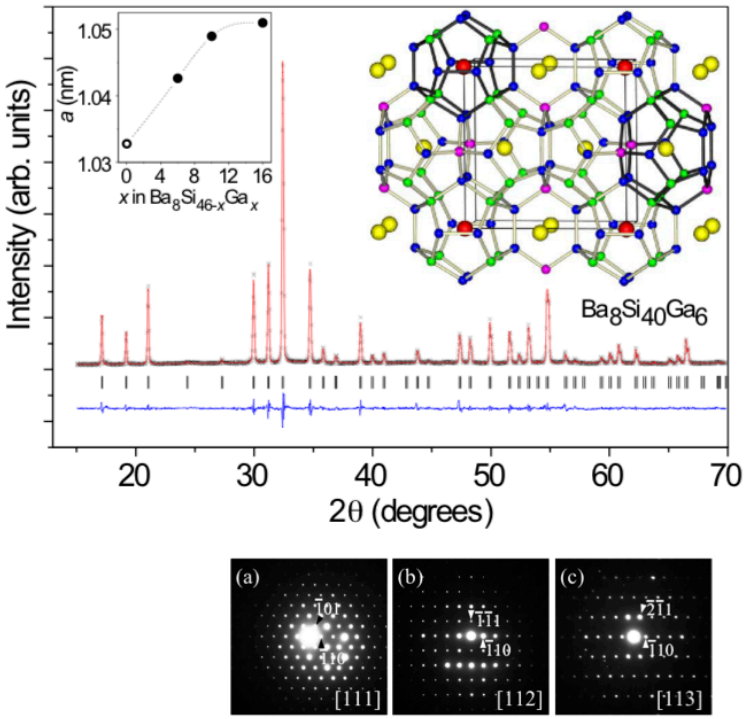


**Figure 1.** Upper figure: Powder x-ray diffraction spectrum, with fitted spectrum after structural refinement, for $Ba_8Si_{40}Ga_6$ (shown in inset). Lower: Three electron diffraction scans for crystallites of the same material, orientations indicated. Ref: Y. Li *et al.*, Phys. Rev. B **75**, 054513 (2007).

**Scattering from crystals:** The concepts used in x-ray scattering include the Bragg formalism as well as that of von Laue, as described in your text. Von Laue's original observation led to his being awarded the 1914 Nobel prize, while William H. and William L. Bragg played a major role in the development of this technique, leading to their being awarded the 1915 Nobel prize.

The **Bragg scattering law** is:

$$n\lambda = 2d\sin\theta. \quad [1]$$

This can be established by considering the crystal planes to be "mirrors" scattering the x-ray beam. Note that since the sin function cannot exceed 1, clearly $\lambda$ must be smaller than $2d$ in order to observe any scattering. The distance $d$ is the spacing of *Bragg planes*, which we have seen is constructed from the *Bravais lattice*, without consideration of the basis. Thus the observed angles are determined by the primitive cell dimensions only, not the positions of basis atoms inside the cell. (The basis atom positions and identities determine the *structure factor*, as shown below, which gives the relative *intensities* of the observed lines.)

**Laue scattering and structure factor:** Consider the incoming and outgoing wavevectors to be $\vec{k}$ and $\vec{k}'$. The scattering angle, $\theta$, is 1/2 the angle between $\vec{k}$ and $\vec{k}'$. We consider each atom to scatter the incoming plane wave into an outgoing *spherical* wave, of amplitude,

$$f_i(\theta)\exp(ik'r)/r\,, \quad [2]$$

where the quantities in the exponent are magnitudes, and the *atomic form factor* $f_i$ contains all the physics of scattering from the $i^{th}$ atom. The scattering is essentially the collected Thomson scattering from the electrons in the atom; similar to Rayleigh scattering from molecules. Note that there is actually another factor such as $(1+\cos^2\theta)$ multiplying the form factor when determining the scattered amplitude; this comes from averaging over the incoming polarizations if the x-ray source tube is not polarized—this doesn't appear in our equations but could easily be added. In any case, the magnitude of $f_i(\theta)$ (which is complex) features a slow decay with increasing angle which depends upon details of the atom.

The detector (at $\vec{r}$) measures a superposition of outgoing spherical waves, emanating from positions $\vec{R}_n + \vec{d}_j$ (Bravais lattice + basis position). The far-field detected waves are essentially parallel, and each has a relative phase

$$\phi = \vec{k}\cdot(\vec{R}_n + \vec{d}_i) + \vec{k}'\cdot(\vec{r} - \vec{R}_n - \vec{d}_i) \equiv \vec{k}'\cdot\vec{r} - \vec{q}\cdot(\vec{R}_n + \vec{d}_i)\,, \qquad [3]$$

where in the middle expression the first term is the phase of the incoming wave reaching the atom, and the second is the further phase picked up along the path to the detector. The term $\vec{k}'\cdot\vec{r}$ on the right is a phase that is the same for all atoms and can be dropped, leaving the last term containing the difference vector defined as $\underline{\vec{q} = \vec{k}' - \vec{k}}$.

To obtain the total amplitude we sum [2] over all atoms in the crystal, with each term multiplied by the appropriate phase factor using [3]. This gives,

$$A(2\theta) \propto \sum_n \sum_j f_j(2\theta)\exp\left(-i\vec{q}\cdot(\vec{R}_n + \vec{d}_j)\right) \propto \int_{cell} d^3r\, n(\vec{r})\exp\left[i(\vec{k} - \vec{k}')\cdot\vec{r}\right]. \quad [4]$$

The expression on the far right in [4] comes about in a scattering-theory picture, since the form factor [2] can be expressed as proportional to a product $\langle\psi_{in}|V(\vec{r})|\psi_{out}\rangle$ joining the incoming and outgoing waves, with the potential $V(r)$ for x-ray interactions simply proportional to the electron density $n$. This result is shown to imphasize the idea that the x-ray scattering amplitude is essentially the <u>Fourier transform of the electron density in the crystal</u>.

In far field we are treating the crystal as a point (same scattering angle for all atoms, which is why there was no index $n$ or $i$ on $\vec{k}'$). So, the sum over $n$ in [4] can be separated into

$$\sum_n \exp\left(-i\vec{q}\cdot\vec{R}_n\right)\,, \qquad [5]$$

multiplied by the sum over $j$, which is independent of $n$. [5] is proportional to $\delta\left(\vec{q} - \vec{K}\right)$ in the infinite crystal limit, as will be discussed in class, with $\vec{K}$ a reciprocal lattice vector. This leads to the <u>*Laue condition*</u>,

$$\vec{q} = \vec{k}' - \vec{k} = \vec{K}\,. \qquad [6]$$

The result shows that elastic scattering occurs <u>only</u> in delta-function-like peaks, at angles $\theta$ where $\vec{k}' - \vec{k} = \vec{K}$. For typical x-ray instruments, the delta-function approximation for [5] works well if the crystal size is 1 $\mu$m or more, otherwise for nano-scale particles the peaks will have an observable width. (This can is sometimes used to measure the size of such small particles).

Putting everything together, we have the amplitude for each scattering peak satisfying [6],

$$A \propto S_{\vec{K}} \equiv \sum_j f_j(2\theta)\exp\left(-i\vec{K}\cdot\vec{d}_j\right). \qquad [7]$$

The expression on the right in [7] is called the *structure factor*. The intensity, measured experimentally, is proportional to the square of [7]. The symmetries of the crystal determine the structure factor and can lead, for example, to systematic zeroes. Determing the set of non-zero peaks allows the space group of the crystal to be identified (out of 230 total space groups), while analyzing the intensities can yield the positions of the atoms.

[Note that I indicated the form factor, $f$, to depend only on one relative angle. In principle this is not completely correct since the atom once it is positioned in the crystal is not spherically symmetric. But, scattering from the core electrons may dominate, and the unmodified atomic form factor is sufficient in many cases. In any event the structure factor [7] *does* require knowledge of the absolute crystal orientation in space because of the factor $\vec{K}$ .]

Examples: Figure 2 shows some of the Bragg planes for the three cubic Bravais lattices. Note that for both BCC and FCC the (100) planes are not included. This occurs because the conventional cubic cell is used to index them, whereas FCC and BCC possess smaller primitive cells. In both cases it is easy to show that the (100) planes do not intersect all lattice sites, so they cannot be a set of Bragg planes. Similar considerations lead to other sets of planes which must be excluded for the BCC and FCC lattices, and thus the "missing peaks" in the corresponding spectra, as shown in Figure 3.

The structure factor [7] yields another way to arrive at the same conclusion, which we will examine in class. For example for the BCC lattice, if we were to view it as a simple cubic lattice with a basis of two identical atoms, $S_{\vec{K}}$ would consists of $f(2\theta)$ multiplied by a factor equal to either 2 or 0. The zeros correspond to indices 100, 111, 210, etc., identical to the missing reflections shown in Fig. 3.

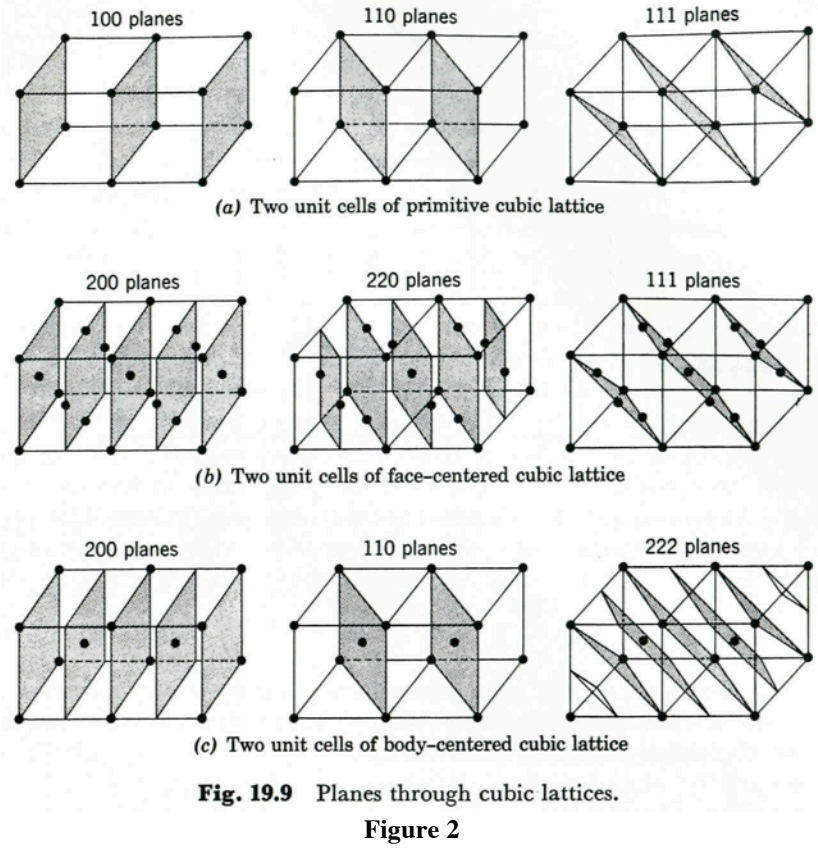


**Figure 2**

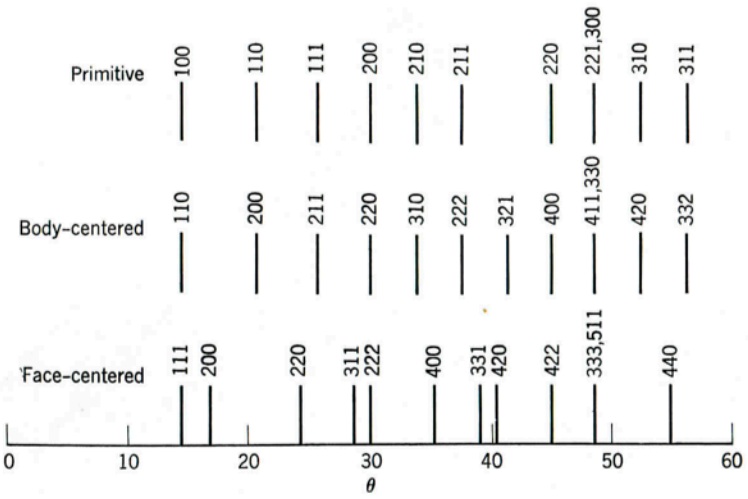


**Fig. 19.10** Angles of incidence $\theta$ and reflection indices from cubic crystals. The values of $\lambda/a$ have been chosen arbitrarily to cause the first reflection to fall at the same angle for each type of crystal. For primitive cubic, $\lambda/a = 0.500$; for body-centered cubic, $\lambda/a = 0.353$; for face-centered cubic, $\lambda/a = 0.289$.

**Figure 3**

**Observation methods:** the condition [6] is difficult to satisfy, such that for a good crystal with random orientation in a narrowly mono-energetic x-ray beam, it is highly unlikely that *any* scattering peaks will be seen. This can be seen by the simple geometrical Ewald construction. However if very finely divided powder is used as the target, a small subset of the crystallites *will* have the proper orientation. With the detector moved in an arc around the sample, peaks will be observed whenever the scattering angle is such that the Laue condition [6] is fulfilled for some of the crystallites. (Or equivalently, the *Bragg condition*, [1], is fulfilled.) This is the powder method, such as was used to generate data for the figure on the second page. For single crystals, a system to rotate or reorient the crystal during measurements is used.

**Remarks:**

*Lattice vibrations* are always present in crystals, so the results of our analysis (for example eqn. [7]) are an idealization. In the early days of x-ray diffraction it had been argued that such effects should completely wash out the spectrum, since at normal temperatures the thermal vibrations give atomic displacements which can be a considerable fraction of the lattice constant, so any "snapshot" one would take of the atoms should show them to be not at all in perfect crystalline order. As it turns out, the perfect-crystal delta functions may still be observed in the presence of such fluctuations, however the scattering peak amplitudes are reduced, and are superposed upon an additional broad background due to phonon scattering. This leads to the Debye-Waller factor, and related effects described in chapter 24.

**References:**

Figure 1 from Y. Li et al., Phys. Rev. B **75**, 054513 (2007). Figures 2 and 3 came from the "Physical Chemistry" textbook [Daniels and Alberty, 1975].